Neuronal genetic rescue normalizes brain network dynamics in a lysosomal storage disorder despite persistent storage accumulation

Authors
Rebecca C. Ahrens-Nicklas*[1,2], Luis Tecedor[3], Arron H. Hall[2], Owen Kane[2], Richard J. Chung[2], Elena Lysenko[3], Eric D. Marsh[4,5], Colleen S. Stein[6], Beverly L. Davidson*[3,7]

Affiliations
[1]Department of Pediatrics, Perelman School of Medicine at the University of Pennsylvania.
[2]Division of Human Genetics, The Children's Hospital of Philadelphia.
[3]The Raymond G. Perelman Center for Cellular and Molecular Therapeutics, The Children's Hospital of Philadelphia.
[4]Department of Neurology, Perelman School of Medicine at the University of Pennsylvania.
[5]Division of Child Neurology, The Children's Hospital of Philadelphia.
[6]Department of Internal Medicine, Fraternal Order of Eagles Diabetes Research Center, Abboud Cardiovascular Research Center, Carver College of Medicine, University of Iowa.
[7]The Department of Pathology and Laboratory Medicine Perelman School of Medicine at the University of Pennsylvania.

*Co-corresponding Authors

Rebecca C. Ahrens-Nicklas, MD, PhD
Children's Hospital of Philadelphia
3615 Civic Center Blvd Abramson 1016H
Philadelphia, PA 19104,
Tel: 215-590-3412
Email: ahrensnicklasr@email.chop.edu

AND

Beverly L. Davidson, PhD
Children's Hospital of Philadelphia,
3501 Civic Center Boulevard, 5060 CTRB,
Philadelphia, PA 19104,
Tel: 267-426-0929,
Email: davidsonbl@chop.edu

Conflicts of interests: BLD is a founder of Spark Therapeutics and Spirovant is on the scientific advisory boards of Intellia Therapeutics, Homology Medicines, Prevail Therapeutics, Resilience, Moment Bio, Spirovant, Saliogen and Panorama Medicines. No other authors report conflicts of interest.

Abstract

Although neurologic symptoms occur in two-thirds of lysosomal storage disorders (LSDs), for most we do not understand the mechanisms underlying brain dysfunction. A major unanswered question is if the pathogenic hallmark of LSDs, storage accumulation, induces functional defects directly or is a disease bystander. Also, for most LSDs we do not know the impact of loss-of-function in individual cell types. Understanding these critical questions are essential to therapy development. Here, we determined the impact of genetic rescue in distinct cell types on neural circuit dysfunction in CLN3 disease, the most common pediatric dementia and a representative LSD. We restored *Cln3* expression via AAV-mediated gene delivery and conditional genetic rescue in a CLN3 mouse model. Surprisingly, we found that low-level rescue of *Cln3* expression in neurons alone normalized clinically-relevant electrophysiologic markers of network dysfunction, despite the presence of substantial residual histopathology, in contrast to restoring expression in astrocytes. Thus loss of Cln3 function in neurons, not storage accumulation, underlies neurologic dysfunction in CLN3 disease, implying that storage clearance may be an inappropriate target for therapy development and an ineffectual biomarker.

Introduction

Lysosomal storage disorders (LSDs) are a group of approximately 50 rare metabolic diseases characterized by progressive accumulation of storage material in lysosomes. Neurological symptoms, including neurocognitive regression, seizures, and psychiatric symptoms, occur in more than 2/3 of LSDs and are generally not ameliorated by current therapies (*1*). For many LSDs, including CLN3 disease, the most common cause of childhood dementia, the mechanisms underlying neurologic dysfunction are poorly understood.

The function of CLN3 protein remains unknown, hindering mechanism-based therapy development. The brains of CLN3 disease mouse models demonstrate progressive storage accumulation, predominantly comprised of subunit C of the mitochondrial ATP synthase (SCMAS) (*2*, *3*), mirroring what occurs in CLN3 disease patients (*4*). Therefore, most drug development efforts rely on histopathologic markers of efficacy, including reduction of storage material, reactive astrocytosis and microgliosis (*2*, *4*, *5*). However, whether these histopathologic changes cause disease, augment the disease process, or are simply harmless epiphenomenon is unclear.

In addition to lack of clarity on the impact of storage, the role of various CNS cell types in driving functional deficits in CLN3 disease is unknown. Astrocytes and microglia isolated from CLN3 disease mouse models demonstrate altered cellular properties and physiology (6-8), and in animal models, localized glial activation occurs in regions where neurons will later die (9) supporting a role for glia as a disease driver. On the other hand, neurons from CLN3 animal models exhibit both histopathologic and functional differences (*2*, *10*, *11*). Ultimately, patients' symptoms such as seizures and neurologic regression arise directly from functional changes in key neuronal circuits. Nonetheless, we do not understand what cell types underlie these pathologic network dynamics in the brain.

Previously, we described network-level neurologic defects in two CLN3 disease mouse models using *in vitro* voltage sensitive dye imaging and *in vivo* electrophysiology techniques (*12*). We found that network-level changes begin early in the disease course before substantial storage accumulation. In slice-recordings, these changes include hypoexcitability of the dentate gyrus of the hippocampus, a region essential for learning and memory. On *in vivo* electroencephalogram (EEG), CLN3 disease mice show frequent epileptiform spikes, a feature of many epilepsy models, and a shift towards high frequency background activity, a change associated with cognitive impairment and present in Alzheimer's disease models and patients (*13*, *14*).

To date, CLN3 disease research has been hindered by the fact that animal models have only subtle behavioral and survival phenotypes (*15*). Most manifest histopathologic changes including storage accumulation and reactive astrocytosis; however, these phenotypes may not correlate with central nervous system (CNS) dysfunction. Our network-level electrophysiologic approach provides a robust, clinically meaningful measure of neurologic function that can probe disease mechanisms and evaluate potential therapies.

Here, we developed a new 'conditional rescue' mouse model of CLN3 disease. The model is homozygous for the most common human CLN3 disease mutation (*2*), but also carries a Cre-inducible wild-type *Cln3* transgene allowing for cell-type specific rescue of expression. We employed AAV-mediated gene replacement as a second strategy to restore *Cln3* expression and combined these tools with network-level electrophysiology techniques to answer three essential questions: 1) Does gene replacement correct neural circuit dysfunction in a LSD? 2) What cell types must be corrected to improve network dynamics? and 3) Does storage accumulation underlie deficits in CNS network dynamics in CLN3 disease?

Results and Discussion

In prior work, we found that CLN3 disease mouse models demonstrate robust, progressive neuronal network defects (*12*). We first assessed if neonatal correction of most CNS cell types could prevent circuit-level functional pathology. For this, we employed an adeno-associated virus serotype 9 (AAV9) vector expressing wild-type murine *Cln3* under control of 1665 bp of the endogenous *Cln3* promoter, which mimics the low levels of expression seen in the endogenous setting **(Sup Figure 1-2, Sup Methods).** Vectors were delivered at p0 via unilateral intracerebroventricular (ICV) infusion into CLN3-deficient mice to transduce both astrocytes and neurons (*16*) **(Sup Figure 3)**. The CLN3 disease mouse model harbors the most common human CLN3 disease mutation, a deletion of exons 7 and 8 ($Cln3^{\Delta ex78/\Delta ex78}$) (*2*). Treatment with AAV9.CLN3 at a dose of $1e^{10}$ vg increased *Cln3* expression **(Figure 1A)**, one year after injection levels in the $Cln3^{\Delta ex78/\Delta ex78}$ hemisphere contralateral to the injection site reached 24.5% ± 4.7 of heterozygous controls. When assessed histologically, gene replacement minimally reduced storage accumulation in both the hippocampus and motor cortex ipsilateral to the injection site **(Figure 1B, Sup Figure 4**).

To determine the impact of p0 AAV9.CLN3 infusion on *in vivo* network dynamics, we recorded activity throughout the brain via *in vivo* EEG. Twelve-month-old $Cln3^{\Delta ex78/\Delta ex78}$ mice have increased spike burden and a shift in background activity towards faster frequencies as compared to $Cln3^{\Delta ex78/WT}$ controls **(Figure 1C-D)**. Specifically, there is decreased power in the slow delta frequency band (0.1-4Hz) and a trend

towards increased power in the faster beta (13-25Hz) and gamma (25-50Hz) bands in *Cln3*$^{\Delta ex78/\Delta ex78}$ mice, consistent with our previous report on *Cln3* knock-out mice (*12*). Remarkably, restoring gene expression at p0 normalized spiking rates **(Figure 1C)** and corrected background activity **(Figure 1D)** in 12-month-old *Cln3*$^{\Delta ex78/\Delta ex78}$ AAV9.CLN3-treated animals. Correction of EEG phenotypes was equally effective in both the hemispheres. Thus, early gene replacement can normalize network dynamics, and this rescue does not require inhibition of storage accumulation.

Because AAV9 delivered to neonates transduces astrocytes and neurons (*16*) it is unclear whether all cell types must be corrected to improve circuit function, a question critically important to translate gene therapies to children; AAV9 delivered into the CNS generally transduces neurons in adult mice and juvenile and adult large animal models (*17-19*). To address this, we developed a conditional rescue model of CLN3 disease, the Flex*Cln3* mouse. This model is homozygous for the common *Cln3* exon 7-8 deletion and also carries the Cre-inducible Flex*Cln3* allele, permitting expression of wild-type Cln3 protein in the presence of Cre recombinase **(Figure 2, Sup Methods and Sup Figures 5-7)**. The Flex*Cln3* allele is under control of the same 1665 bp *Cln3* promoter as used for AAV-mediated gene replacement.

We validated the model by crossing Flex*Cln3* mice with *Zp3-Cre* mice (*20*) to drive germline level recombination and flip the reverse-oriented wildtype Flex*Cln3* allele into the forward orientation in all cells. In these mice *Cln3* expression was ubiquitously restored, with expression levels dictated by the transgenic *Cln3* 1665 bp promoter. *Cln3* expression in the hippocampus was restored to 30.5% of heterozygous (*Cln3*$^{\Delta ex78/WT}$) control levels as determined by qPCR. For selective rescue of astrocytes or neurons, Flex*Cln3* mice were crossed to *Gfap-Cre* (21) or *Syn1-Cre* (22) drivers, respectively. Expression of forward-oriented Flex*Cln3* transcripts was confirmed in the hippocampus of animals for all three rescue conditions: restoration to "all cells" (Flex*Cln3*/ *Cln3*$^{\Delta ex78/\Delta ex78}$/ *Zp3-Cre*), astrocytes (Flex*Cln3* / *Cln3*$^{\Delta ex78/\Delta ex78}$ / *Gfap-Cre* mice), and neurons (Flex*Cln3* / *Cln3*$^{\Delta ex78/\Delta ex78}$ / *Syn1-Cre*). **(Figure 2C)**.

We next determined the impact of cell type-selective restoration of *Cln3* on histopathological and electrophysiologic readouts. Correction in all cell types substantially reduced SCMAS storage in the hippocampus and other brain regions **(Figure 2B, Sup Figure 8)**. Rescue of *Cln3* expression in either astrocytes (Flex*Cln3* / *Cln3*$^{\Delta ex78/\Delta ex78}$ / *Gfap-Cre*) or neurons (Flex*Cln3* / *Cln3*$^{\Delta ex78/\Delta ex78}$ / *Syn1-Cre*) alone did not prevent storage accumulation in the hippocampus or motor cortex in 6 or 12-month-old mice **(Figure 2D-M, Sup Figures 8-9)**. In addition to storage accumulation, CLN3 disease mice develop

progressive, reactive astrocytosis. At twelve months of age, both the hippocampus and motor cortex of *Cln3*$^{\Delta ex78/\Delta ex78}$ showed increased astrocytosis as compared to wild-type controls. Rescue of *Cln3* expression in either neurons or astrocytes alone did not prevent astrocytosis **(Sup Figure 10)**.

In vitro voltage sensitive dye imaging of hippocampal slices from 6-month-old animals was completed in Flex*Cln3* / *Cln3*$^{\Delta ex78/\Delta ex78}$ / *Gfap-Cre*, Flex*Cln3* / *Cln3*$^{\Delta ex78/\Delta ex78}$ / *Syn1-Cre, and FlexCln/Cln3*$^{\Delta ex78/\Delta ex78}$ /Zp3 mice. In this early-stage of disease, the internal blade of the dentate gyrus of the *Cln3*$^{\Delta ex78/\Delta ex78}$ hippocampus was hypoexcitable in response to perforant path stimulation as compared to heterozygous *CLN3*$^{\Delta 78/WT}$ mice **(Figure 3A-C)**, consistent with our previous studies (*12*). Specifically, 32.7% of pixels in the internal blade of the *Cln3*$^{\Delta ex78/\Delta ex78}$ dentate gyrus were significantly hypoexcitable as compared to slices obtained from heterozygous control animals. Interestingly, restoring expression in astrocytes did not correct hypoexcitability of the dentate gyrus **(Figure 3D-E)**. However, restoring *Cln3* expression in neurons was sufficient to prevent disease-induced hypoexcitability **(Figure 3F-G)**, in fact excitability was mildly increased as compared to controls. This rescue of dynamics occurred despite the presence of residual histopathology **(Figure 2 and Sup. Figures 8-9)**.

To evaluate cell-type correction requirements on CNS functional defects *in vivo,* we measured network activity through long-term EEG recordings. While restoration of Cln3 in either astrocytes or neurons prevented epileptiform spikes throughout the brain (**Figure 4A**), only rescue in neurons corrected EEG background frequency composition and thereby fully normalized network activity **(Figure 4B-C)**. Intriguingly, this correction of physiology occurred despite the presence of substantial storage burden, revealing for the first time that loss of Cln3 protein function in neurons, not storage burden, underlies functional defects in CLN3 disease.

Previous cellular-level studies of CLN3 disease have demonstrated disease-associated abnormalities in both neurons and astrocytes (4, 7-9, 11, 23, 24). Prior to this work, it was unknown how these cellular defects translate to the circuit-level dysfunction that underlies neurological symptoms such as dementia and seizures that CLN3 disease patients experience. This work highlights the fact that neurons underlie functional defects in CLN3 disease and must be targeted in future drug development efforts.

A number of novel therapies, including small molecule (5, 25-29), antisense oligonucleotides (30), and gene replacement (31, 32) strategies are under development for CLN3 disease. These approaches will not target all cell types equally. For example, studies in non-human primates have demonstrated that intravenous administration of AAV9 in juvenile non-human primates predominately transduces glia (19,

33) while direct administration into the cerebral spinal fluid (CSF) improves delivery to neurons (34). Our results suggest that maximizing neuronal correction will be essential to develop a treatment that improves functional outcomes in CLN3 disease.

In previous studies, *Cln3*$^{\Delta ex78/\Delta ex78}$ mice have demonstrated abnormal astrocytic-neuronal coupling (7). Monogenic mouse models of isolated astrocyte dysfunction have epileptiform spikes and seizures on EEG because of pathologic cross-talk between astrocytes and neurons (35). In the Flex*Cln3* mouse, while rescue of *Cln3* expression in astrocytes did not normalize EEG background, it was sufficient to prevent epileptiform spikes. The reduction in spiking likely reflects improved astrocytic-neuronal interactions when *Cln3* expression is restored in astrocytes. Collectively, our data suggests that diseased astrocytes may modulate network-level dysfunction in CLN3 disease, but diseased neurons are the primary driver of functional deficits.

Using our cell-type specific rescue model, we found that storage accumulation was prevented when *Cln3* was re-introduced to all cell types embryonically, but not when that correction was restricted to astrocytes or neurons alone. Interestingly, prevention of storage accumulation is not required for correcting neuronal network physiology, suggesting that storage material does not underlie functional defects and may be an innocent bystander in the disease process. These studies highlight the importance of using clinically-relevant functional measures, such as *in vivo* electrophysiology studies, to guide treatment development. Histologic measures, such as storage burden, may be poor surrogate biomarkers of therapeutic efficacy in CLN3 disease and possibly other neuronopathic LSDs.

In summary, partial restoration of Cln3 expression by AAV vectors or through Cre-based systems shows that neuronal expression is critical for preventing deficits in CNS functional circuits in CLN3 disease mice. This work also highlights that improvement in storage burden may be a poor readout of therapeutic efficacy in CLN3 disease, a phenomenon that should be considered by the broader LSD community.

Materials and Methods

For additional information, see Supplemental Methods. *Study approval:* All animal protocols were approved by the Institutional Animal Care and Use Committee at the Children's Hospital of Philadelphia.

Acknowledgments: NINDS R21NS084424 and NICHD HD33532 to BLD, NIH K08NS105865 to RAN, NCL Stiftung Research Award to RAN, Children's Hospital of Philadelphia Research Institute support to RAN and BLD.

Author contributions:
Design of study: RA, LT, AH, OK, RC, EL, EM, CS, BD

Data acquisition and analysis of data: RA, LT, AH, OK, RC, EL, CS
Drafting of manuscript: RA, LT, AH, OK, CS
Critical review of data and manuscript: RA, LT, EM, CS, BD

Figures

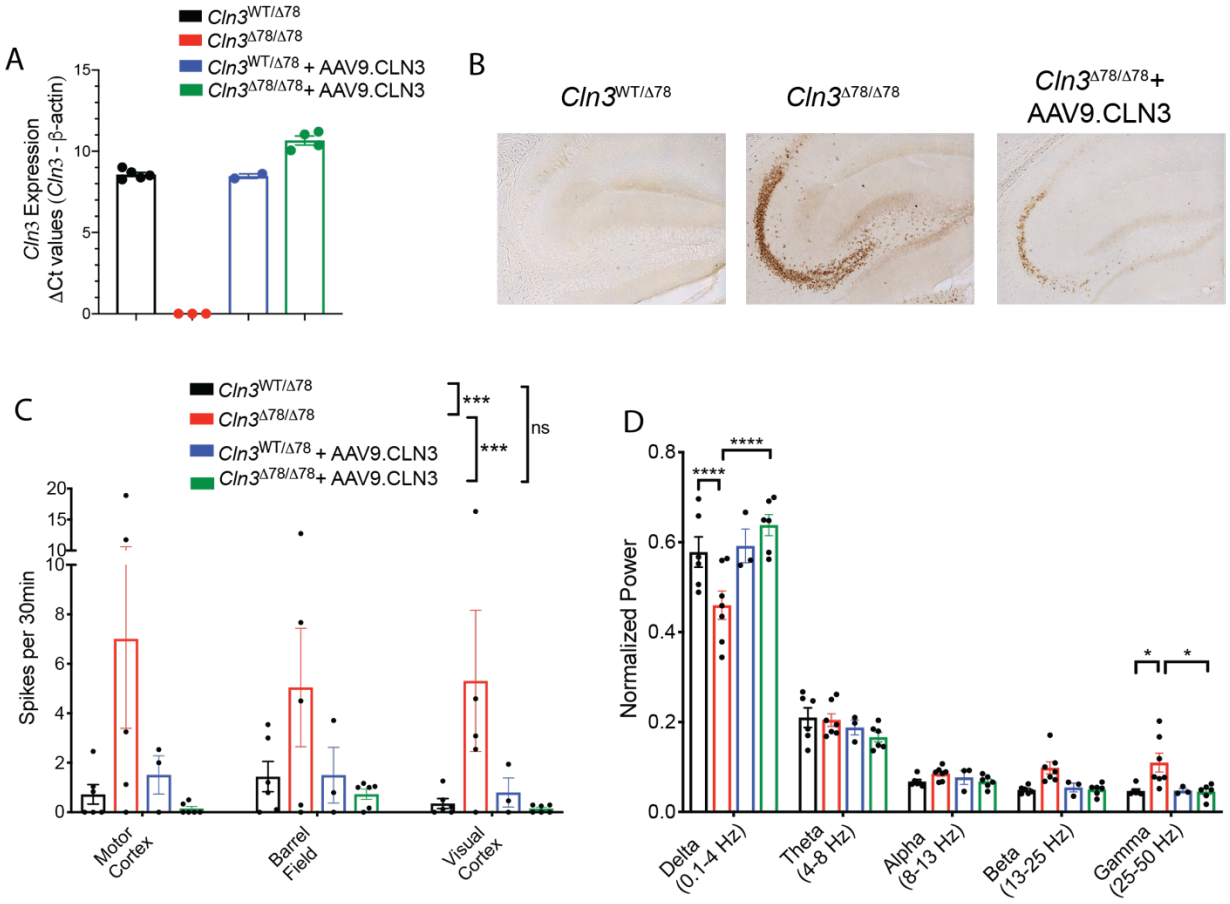

Figure 1: Intracerebroventricular AAV9.CLN3 gene therapy given at p0 normalizes neuronal network dynamics *in vivo* at 12 months of age. (A) p0 ICV injection of AAV9.CLN3 restored CLN3 expression in $Cln3^{\Delta ex78/\Delta ex78}$ mouse brain at 12 months of age, with levels in the $Cln3^{\Delta ex78/\Delta ex78}$ hemisphere contralateral to the injection site reaching 24.5% ± 4.7 of heterozygous controls. **(B)** Subunit C accumulation is partially corrected in the hippocampus ipsilateral to the injection site of $Cln3^{\Delta ex78/\Delta ex78}$ mice treated with AAV9.CLN3. Gene replacement corrects circuit function measured on intracranial EEG including **(C)** epileptiform spiking rates in throughout the cortex and **(D)** background frequency composition in the motor cortex. Groups: $Cln3^{WT/\Delta ex78}$ (black); $Cln3^{\Delta ex78/\Delta ex78}$ (red); $Cln3^{WT/\Delta ex78}$ + AAV9.CLN3 (blue); $Cln3^{\Delta ex78/\Delta ex78}$ + AAV9.CLN3 (green). N=4-5 animals/condition, analyzed by two-way ANOVA by band and genotype, followed by Sidak's multiple comparisons test. *p<0.05, **p<0.01, ***p<0.001, ****p<0.0001.

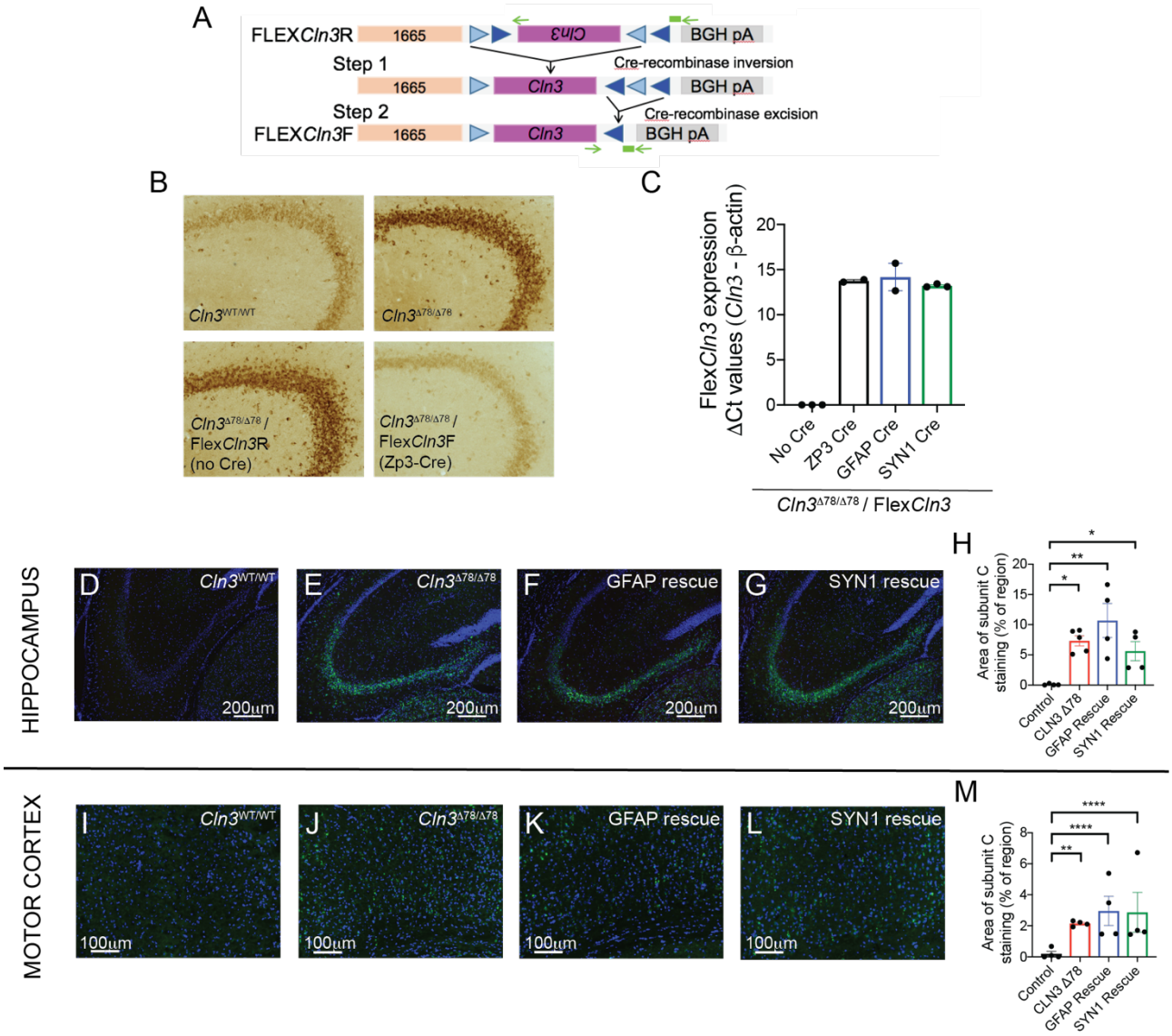

Figure 2: Expression of Flex*Cln3* allele in all cell types prevents storage accumulation, while expression in either neurons or astrocytes alone does not. (A) In the presence of Cre, the Flex*Cln3* allele undergoes inversion (Step 1) and excision (Step 2) and is expressed under control of its endogenous promoter. **(B)** Subunit C of the mitochondrial ATP synthase (SCMAS) accumulates in the hippocampus of $Cln3^{\Delta ex78/\Delta ex78}$ and Flex*Cln3* / $Cln3^{\Delta ex78/\Delta ex78}$ mice. Storage is reduced in mice with the Flex*Cln3* allele in the forward confirmation. **(C)** Flex*Cln3* expression is not detected by quantitative PCR in the hippocampus of Flex*Cln3* / $Cln3^{\Delta ex78/\Delta ex78}$ mice in the absence of Cre recombinase. However, there is Flex*Cln3* expression in the hippocampus in the presence of the *Zp3*-Cre (black, ubiquitous rescue), *Gfap*-Cre (blue, astrocyte rescue) or *Syn1*-Cre (green, neuronal rescue) **(D)** The CA3 region of twelve-month-old $Cln3^{WT/WT}$ hippocampus demonstrates little SCMAS storage (green), as compared to **(E)** $Cln3^{\Delta ex78/\Delta ex78}$ hippocampus. **(F-H)** Expression of Flex*Cln3* in astrocytes (Flex*Cln3* / $Cln3^{\Delta ex78/\Delta ex78}$ / *Gfap*-Cre animals) or neurons alone (Flex*Cln3* / $Cln3^{\Delta ex78/\Delta ex78}$ / *Syn1*-Cre animals) does not prevent storage accumulation. **(I-M)** Similar findings were seen in the motor cortex. N=4-5 animals, two-way ANOVA by animal and genotype, followed by Holm-Sidak's or Tukey's multiple comparisons test. For all panels: *$p<0.05$, **$p<0.01$, ***$p<0.001$, ****$p<0.0001$.

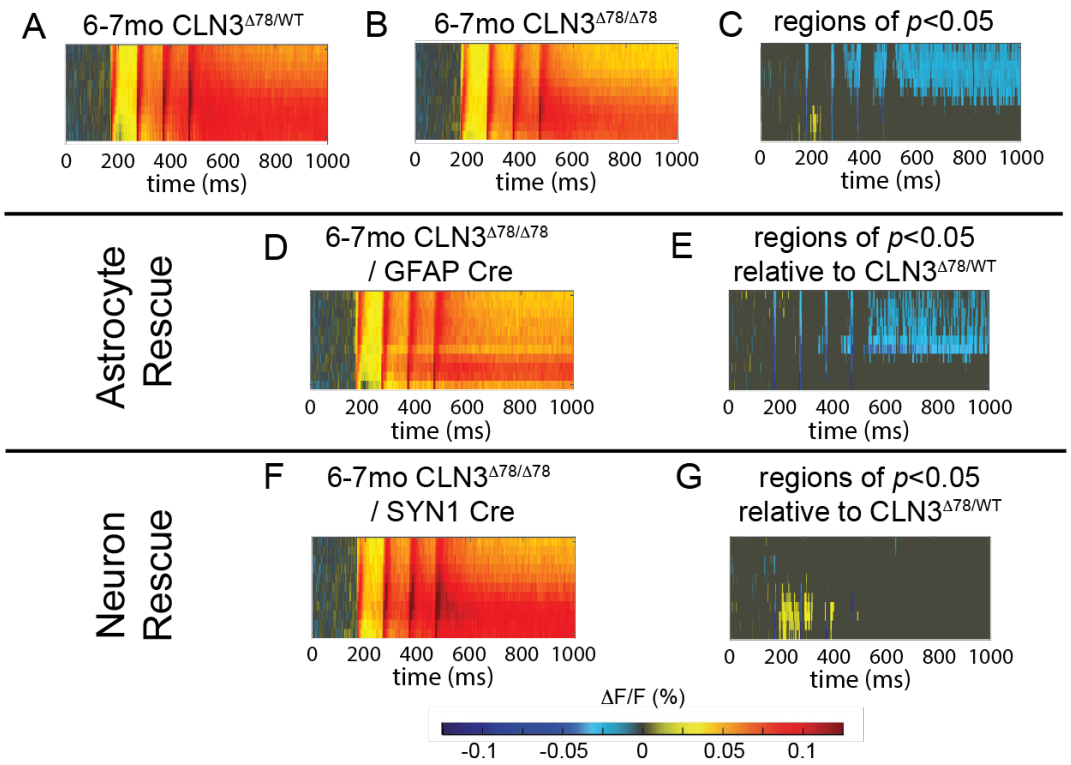

Figure 3: Restoring low level *Cln3* expression in neurons alone corrects hypoexcitability of the dentate gyrus. Dentate gyrus excitability measured through *in vitro* voltage sensitive dye imaging of hippocampal slices from 6-month old animals is shown as raster plots of average fluorescence change (ΔF/F warm colors excitation, cool colors inhibition) over time (X axis) and location within the internal blade of the dentate gyrus (Y Axis). **(A)** Four-pulse stimulation of the perforant path in heterozygous control ($Cln3^{\Delta ex78/WT}$) mice reveals robust excitation of the dentate gyrus (DG) as compared to **(B)** $Cln3^{\Delta ex78/\Delta ex78}$ mice**. (C)** $Cln3^{\Delta ex78/WT}$ vs. $Cln3^{\Delta ex78/\Delta ex78}$ rasters were compared using a permutation sampling method. Pixels with $p>0.05$ are masked in gray. For regions of significance with $p<0.05$, the difference in fluorescence change ($\Delta F/F_{\Delta ex78/WT}$ -$\Delta F/F_{\Delta ex78/\Delta ex78}$) is shown. **(D-E)** In animals expressing *Cln3* in astrocytes (Flex*Cln3* / $Cln3^{\Delta ex78/\Delta ex78}$ / *Gfap*-Cre), the DG remained hypoexcitable as compared to the $Cln3^{\Delta ex78/WT}$ DG. **(F-G)** Expression of *Cln3* in neurons alone (Flex*Cln3* / $Cln3^{\Delta ex78/\Delta ex78}$ / *Syn1*-Cre) was sufficient to reverse hypoexcitability of the DG as compared to $Cln3^{\Delta ex78/WT}$ animals. Group sizes (n=slices, N=mice): $Cln3^{\Delta ex78/WT}$ n= 23 N=4; $Cln3^{\Delta ex78/\Delta ex78}$ n= 30, N=6; Flex*Cln3* / $Cln3^{\Delta ex78/\Delta ex78}$ / *Gfap-Cre* n=19 slices, N=4; Flex*Cln3* / $Cln3^{\Delta ex78/\Delta ex78}$ / *Syn1-Cre* n=17; N=4.

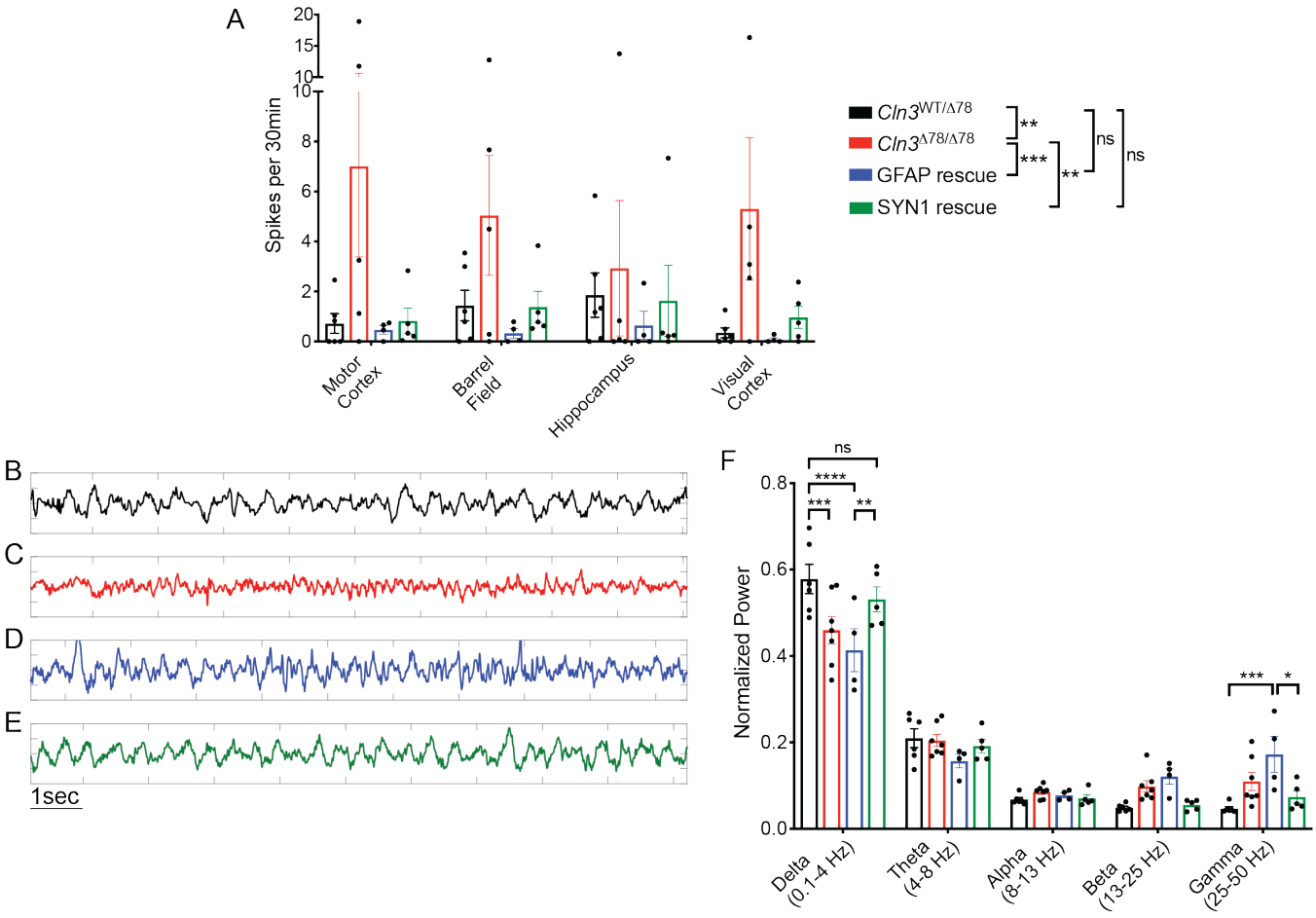

Figure 4: Cln3 rescue in either astrocytes or neurons reduces epileptiform spikes, but only neuronal rescue fully normalizes network dynamics as measured on EEG. (A) Correction of either astroctyes (Flex*Cln3* / *Cln3*$^{\Delta ex78/\Delta ex78}$ / *Gfap*-Cre, blue) or neurons (Flex*Cln3* / *Cln3*$^{\Delta ex78/\Delta ex78}$ / *Syn1*-Cre, green) reduced spike burden on EEG in 12 month old mice. **(B-E)** Example EEG traces from *Cln3*$^{\Delta ex78/\Delta ex78}$ (red) and Flex*Cln3* / *Cln3*$^{\Delta ex78/\Delta ex78}$ / *Gfap*-Cre motor cortex (blue) show decreased slow delta activity and increased fast activity as compared to control motor cortex (black). EEG trace from Flex*Cln3* / *Cln3*$^{\Delta ex78/\Delta ex78}$ / *Syn1*-Cre motor cortex (green) shows that rescue of *Cln3* expression in neurons normalizes EEG background frequency composition. **(F)** Power spectral analysis of EEG data recorded in the motor cortex confirms that rescue of *Cln3* expression in astrocytes (blue) does not correct disease-associated loss of delta activity, and actually exacerbates increased fast gamma activity. However, correction in neurons (green) normalizes EEG frequency composition. N=4-5 animals/genotype, analyzed by two-way ANOVA by band and genotype, followed by Sidak's multiple comparisons test. *$p<0.05$, **$p<0.01$, ***$p<0.001$.

References

1. Platt FM. Emptying the stores: lysosomal diseases and therapeutic strategies. *Nat Med* 2017;17(2):133–150.

2. Cotman SL et al. Cln3(Deltaex7/8) knock-in mice with the common JNCL mutation exhibit progressive neurologic disease that begins before birth. *Hum. Mol. Genet.* 2002;11(22):2709–2721.

3. Eliason SL et al. A knock-in reporter model of Batten disease. *J. Neurosci.* 2007;27(37):9826–9834.

4. Tyynelä J, Cooper JD, Khan MN, Shemilts SJA, Haltia M. Hippocampal pathology in the human neuronal ceroid-lipofuscinoses: distinct patterns of storage deposition, neurodegeneration and glial activation. *Brain Pathol.* 2004;14(4):349–357.

5. Tarczyluk-Wells MA et al. Combined Anti-inflammatory and Neuroprotective Treatments Have the Potential to Impact Disease Phenotypes in Cln3−/− Mice. *Front. Neurol.* 2019;10:107–10.

6. Xiong J, Kielian T. Microglia in juvenile neuronal ceroid lipofuscinosis are primed toward a pro-inflammatory phenotype. *J. Neurochem.* 2013;127(2):245–258.

7. Burkovetskaya M et al. Evidence for Aberrant Astrocyte Hemichannel Activity in Juvenile Neuronal Ceroid Lipofuscinosis (JNCL). *PLoS ONE* 2014;9(4):e95023.

8. Parviainen L et al. Glial cells are functionally impaired in juvenile neuronal ceroid lipofuscinosis and detrimental to neurons. *Acta Neuropathol Commun* 2017;5(1):74.

9. Pontikis CC et al. Late onset neurodegeneration in the Cln3-/- mouse model of juvenile neuronal ceroid lipofuscinosis is preceded by low level glial activation. *Brain Res.* 2004;1023(2):231–242.

10. Brenneman DE, Pearce DA, Kovacs A, DeFrees S. Pharmacological Effects on Ceroid Lipofuscin and Neuronal Structure in Cln3 Δex7/8 Mouse Brain Cultures. *J. Mol. Neurosci.* 2017;63(1):100–114.

11. Grünewald B et al. Defective synaptic transmission causes disease signs in a mouse model of juvenile neuronal ceroid lipofuscinosis. *Elife* 2017;6:621.

12. Ahrens-Nicklas RC et al. Neuronal network dysfunction precedes storage and neurodegeneration in a lysosomal storage disorder. *JCI Insight* 2019;4(21):e131961.

13. Kwak YT. Quantitative EEG findings in different stages of Alzheimer's disease. *J Clin Neurophysiol* 2006;23(5):456–461.

14. Kent BA, Strittmatter SM, Nygaard HB. Sleep and EEG Power Spectral Analysis in Three Transgenic Mouse Models of Alzheimer's Disease: APP/PS1, 3xTgAD, and Tg2576. *J Alzheimers Dis* 2018;64(4):1325–1336.

15. Faller KME et al. The neuronal ceroid lipofuscinoses: Opportunities from model systems. *BBA - Molecular Basis of Disease* 2015;1852(PB):2267–2278.

16. Hammond SL, Leek AN, Richman EH, Tjalkens RB. Cellular selectivity of AAV serotypes for gene delivery in neurons and astrocytes by neonatal intracerebroventricular injection. *PLoS ONE* 2017;12(12):e0188830.

17. Hinderer C et al. Widespread gene transfer in the central nervous system of cynomolgus macaques following delivery of AAV9 into the cisterna magna. *Mol Ther Methods Clin Dev* 2014;1:14051.

18. Gray SJ, Nagabhushan Kalburgi S, McCown TJ, Jude Samulski R. Global CNS gene delivery and evasion of anti-AAV-neutralizing antibodies by intrathecal AAV administration in non-human primates. *Gene Ther* 2013;20(4):450–459.

19. Samaranch L et al. Adeno-associated virus serotype 9 transduction in the central nervous system of nonhuman primates. *Human Gene Therapy* 2012;23(4):382–389.

20. Shafi R et al. The O-GlcNAc transferase gene resides on the X chromosome and is essential for embryonic stem cell viability and mouse ontogeny. *Proc Natl Acad Sci USA* 2000;97(11):5735–5739.

21. Gregorian C et al. Pten deletion in adult neural stem/progenitor cells enhances constitutive neurogenesis. *J. Neurosci.* 2009;29(6):1874–1886.

22. Zhu Y et al. Ablation of NF1 function in neurons induces abnormal development of cerebral cortex and reactive gliosis in the brain. *Genes Dev.* 2001;15(7):859–876.

23. Pontikis CC, Cotman SL, MacDonald ME, Cooper JD. Thalamocortical neuron loss and localized astrocytosis in the Cln3Deltaex7/8 knock-in mouse model of Batten disease. *Neurobiol. Dis.* 2005;20(3):823–836.

24. Bosch ME, Kielian T. Astrocytes in juvenile neuronal ceroid lipofuscinosis (CLN3) display metabolic and calcium signaling abnormalities. *J. Neurochem.* 2019;148(5):612–624.

25. Schultz ML et al. Modulating membrane fluidity corrects Batten disease phenotypes in vitro and in vivo. *Neurobiol. Dis.* 2018;115:182–193.

26. Augustine EF et al. Short-Term Administration of Mycophenolate Is Well-Tolerated in CLN3 Disease (Juvenile Neuronal Ceroid Lipofuscinosis). In: *JIMD Reports, Volume 23*. Berlin, Heidelberg: Springer Berlin Heidelberg; 2018:117–124

27. Sitt El S et al. Exogenous Galactosylceramide as Potential Treatment for CLN3 Disease. *Ann Neurol.* 2019;86(5):729–742.

28. Petcherski A et al. An Autophagy Modifier Screen Identifies Small Molecules Capable of Reducing Autophagosome Accumulation in a Model of CLN3-Mediated Neurodegeneration. *Cells* 2019;8(12):1531.

29. Maalouf K et al. Exogenous Flupirtine as Potential Treatment for CLN3 Disease. *Cells* 2020;9(8):1872.

30. Centa JL et al. Therapeutic efficacy of antisense oligonucleotides in mouse models of CLN3 Batten disease. *Nat Med* 2020;26(9):1444–1451.

31. Bosch ME et al. Self-Complementary AAV9 Gene Delivery Partially Corrects Pathology Associated with Juvenile Neuronal Ceroid Lipofuscinosis (CLN3). *J. Neurosci.* 2016;36(37):9669–9682.

32. kleine Holthaus S-M et al. Gene Therapy Targeting the Inner Retina Rescues the Retinal Phenotype in a Mouse Model of CLN3 Batten Disease. *Human Gene Therapy* 2020;31(13-14):709–718.

33. Gray SJ et al. Preclinical differences of intravascular AAV9 delivery to neurons and glia: a comparative study of adult mice and nonhuman primates. *Mol. Ther.* 2011;19(6):1058–1069.

34. Bey K et al. Intra-CSF AAV9 and AAVrh10 Administration in Nonhuman Primates: Promising Routes and Vectors for Which Neurological Diseases? *Mol Ther Methods Clin Dev* 2020;17:771–784.

35. Robel S et al. Reactive astrogliosis causes the development of spontaneous seizures. *J. Neurosci.* 2015;35(8):3330–3345.